
Since January 2020 Elsevier has created a COVID-19 resource centre with free information in English and Mandarin on the novel coronavirus COVID-19. The COVID-19 resource centre is hosted on Elsevier Connect, the company's public news and information website.

European Journal of Medicinal Chemistry 66 (2013) 314–323

Contents lists available at SciVerse ScienceDirect

European Journal of Medicinal Chemistry

journal homepage: http://www.elsevier.com/locate/ejmech

Original article

# Synthesis of 4-aminoquinoline–pyrimidine hybrids as potent antimalarials and their mode of action studies

Kamaljit Singh [a,*], Hardeep Kaur [a], Kelly Chibale [b], Jan Balzarini [c]

[a] Department of Chemistry, UGC-Centre of Advance Study-1, Guru Nanak Dev University, Amritsar, Punjab 143005, India
[b] Department of Chemistry, Institute of Infectious Disease and Molecular Medicine, University of Cape Town, Rondebosch 701, South Africa
[c] Rega Institute for Medical Research, KU Leuven, Minderbroedersstraat 10, B-3000 Leuven, Belgium

ARTICLE INFO

*Article history:*
Received 6 May 2013
Received in revised form
29 May 2013
Accepted 30 May 2013
Available online 10 June 2013

*Keywords:*
Antimalarials
4-Aminoquinolines
Heme binding
Hybrid molecules
Drug discovery

ABSTRACT

One of the most viable options to tackle the growing resistance to the antimalarial drugs such as artemisinin is to resort to synthetic drugs. The multi-target strategy involving the use of hybrid drugs has shown promise. In line with this, new hybrids of quinoline with pyrimidine have been synthesized and evaluated for their antiplasmodial activity against both $CQ^S$ and $CQ^R$ strains of *Plasmodium falciparum*. These depicted activity in nanomolar range and were found to bind to heme as well as AT rich pUC18 DNA.



## 1. Introduction

Malaria is one of the most widespread diseases besides tuberculosis and AIDS which affects more than 500 million people worldwide and results in around 1–3 million causalities every year [1]. In Africa alone, around 20% childhood deaths are due to malaria and a child dies every 30 s [2] and it is estimated that an African child has on an average 1.6–5.4 episodes of malaria fever each year. Of the four typically recognized *Plasmodium* species causing disease in humans, *Plasmodium falciparum* is most deadly to children below the age of five leading to mortality while *Plasmodium vivax* is most morbidity prone, and is responsible for latent infection that hampers current control and future elimination efforts [3]. The development of drug resistance for the common antimalarials such as 4-/8-aminoquinolines, 4-methanol quinolines, antifolate drugs, sesquiterpene lactones etc. (Fig. 1) is a rather serious issue which has stimulated considerable research efforts in the development of new drugs using different approaches [4,5] of which the molecular hybridization approach [6,7] is quite an attractive strategy which involves design of new chemical entities by covalent fusion of two drugs, both active compounds and/or pharmacophoric units derived from known bioactive molecules with complimentary activities and multiple pharmacological targets. The multiple target strategy led to the design of hybrid of 4-aminoquinoline with species such as triazine [8,9], ferrocene [10], rhodanine [11], thiazolidine-4-one [12], chalcone [13], trioxane [14], isatin [15] and recently, pyrimidines [16–18] (Fig. 2).

Quinoline containing drugs (chloroquine and primaquine, Fig. 1) are known to affect parasite metabolism and cause parasite death by blocking the polymerization of the toxic heme, into an insoluble and non-toxic pigment, hemozoin, resulting in cell lysis and parasite cell auto digestion [19–21]. On the other hand, pyrimidine-based compounds are well known for their wide range of promising antiviral [22], antitubercular [23], anti-AIDS [24], antinociceptive [25], antifungal [26], antitumor [27] and antimalarial activities [28] apart from their role in the nucleic acid synthesis. Thus, linking of the quinoline unit with pyrimidine might furnish conjugate hybrids that are capable of showing useful antimalarial activity.

Recently, antimalarial activities of some quinoline–pyrimidine hybrids with activities in the micromolar to nanomolar range have been reported (Fig. 3) [16–18,29]. In yet another report on the evaluation of quinoline–pyrimidine, the activity (in micromolar range) was also reported for fixed combinations of the chloroquine and pyrimethamine. In all these reports, the pyrimidines were linked to the quinoline unit through 2-, 4- and 6-positions. We have employed

* Corresponding author. Tel.: +91 183 2258853; fax: +91 183 2258819/20.
*E-mail addresses:* kamaljit19in@yahoo.co.in, kamaljitgndu@gmail.com (K. Singh).

0223-5234/$ – see front matter © 2013 Elsevier Masson SAS. All rights reserved.
http://dx.doi.org/10.1016/j.ejmech.2013.05.046

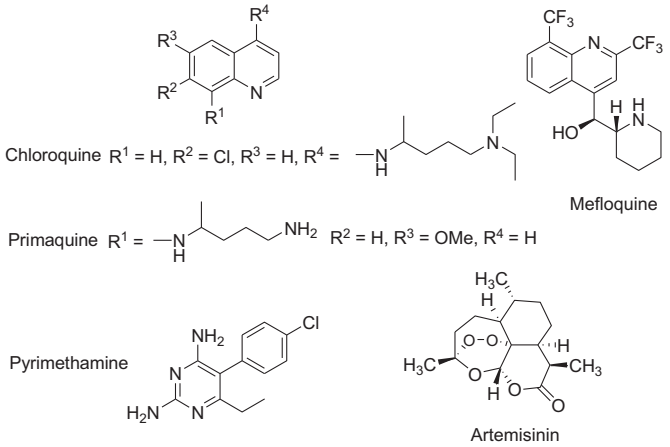


**Fig. 1.** Small molecule antimalarial agents.

rather conformationally flexible pyrimidine-5-carboxylates linked covalently to 4-aminoquinoline core. These novel pyrimidine carboxylate hybrids interact with the iron center of free heme within the physiological environment (pH 5.6), a key step in the accumulation of heme which is selectively toxic to the parasite. To enhance the possibility to accumulate within the digestive vacuole *via* weak-base trapping (the mechanism by which CQ and other quinoline antimalarials attain high concentrations inside this compartment), we developed a novel class of antimalarials using a pharmacophore hybridization approach in which the pyrimidine-5-carboxylate motif was hybridized with an iron-complexing, 4-aminoquinoline moiety through C-2 position [29]. To further elaborate the structure–activity profile, here, we present additional new 4-aminoquinoline–pyrimidine carboxylate hybrids. We also report on their antimalarial activity against both CQ sensitive ($CQ^S$ Dd2) as well as CQ resistant ($CQ^R$ D10) strains. Finally, the mechanism of action studies with the representative compounds has also been performed.

## 2. Chemistry

The 4-aminoquinoline–pyrimidine-5-carboxylate hybrids were synthesized in economical way using synthetic approach outlined in Scheme 1. The key starting compound, 3,4-dihydropyrimidin-2(1H)-one **1** was prepared through $NH_4Cl$/TFA [30,31] catalyzed three-component Biginelli condensation of an alkyl acetoacetate, urea and appropriate aldehyde or its formyl equivalent: 1,3-oxazinane derivative, in acetonitrile or under solvent-free reaction conditions, in some cases. Subsequent oxidation of **1** using 60% nitric acid readily furnished pyrimidinones **2** which upon chlorination with $POCl_3$ yielded **3** [32]. The nucleophilic substitution reaction of **3** with appropriate 4-amino-7-chloroquinoline **4** which in turn was prepared from the commercially available 4,7-dichloroquinoline and diaminoalkanes [33], gave **5a**–**g** in good yields (Table 1). Structures of **1**–**5** were unambiguously established on the basis of spectral ($^1$H NMR, $^{13}$C NMR, MS, FT IR) as well as microanalytical analysis.

## 3. Results and discussion

### 3.1. Antimalarial activity and structure–activity relationships (SARs)

We have previously established that the 4-aminoquinoline–pyrimidine hybrids **6a**–**c** intercepted by a diaminoalkyl spacer showed optimum potency (Table 1), when the flexible spacer consisted of three or four carbon atoms [29]. Further, the introduction of nitro substituent at ortho position of the phenyl ring at the C-4 of the pyrimidine core furnished the most potent compound **6c** with antimalarial activity superior to the standard CQ and close to artesunate [29]. Keeping these observations in mind, we planned to further refine the activity of these persuasive 4-aminoquinoline–pyrimidine by incorporating electron withdrawing substituents at C-4 phenyl of pyrimidine core, as well as by varying the C-5 ester substituent and also by altering the basicity of diaminoalkyl spacer.

The *in vitro* antimalarial screening of the new synthesized compounds **5a**–**g** revealed good to moderate activities in nM range against both the tested Dd2 ($CQ^S$) and D10 strains ($CQ^R$) of *P. falciparum* (Table 1). Although the tested hybrids were not as active as the standard drugs *viz*. CQ and ASN, interesting SARs have been drawn. Analysis of the activity of the compounds recorded in Table 1 reveals that replacing C-5 ethyl ester of the previously reported [29] compound **6a** [$IC_{50}$ 247.5 nM ($CQ^S$); 52.2 nM ($CQ^R$)] with methyl ester **5a** [$IC_{50}$ 659 nM ($CQ^S$); 542 nM ($CQ^R$)] led to the

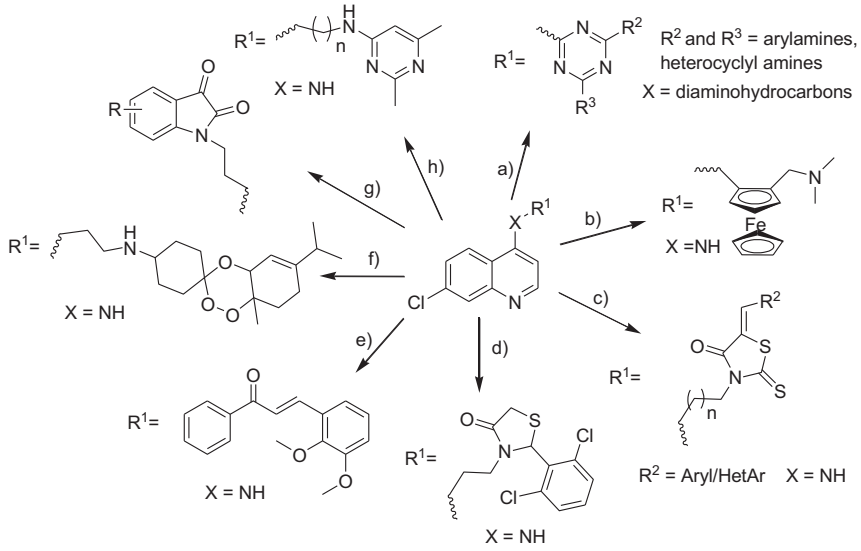


**Fig. 2.** Representative designs of 4-aminoquinoline based hybrid drugs showing antimalarial activity (quinoline hybrids with (a) triazine, (b) ferrocene, (c) rhodanine, (d) thiazolidin-4-one, (e) chalcone, (f) trioxane, (g) isatin and (h) pyrimidine).

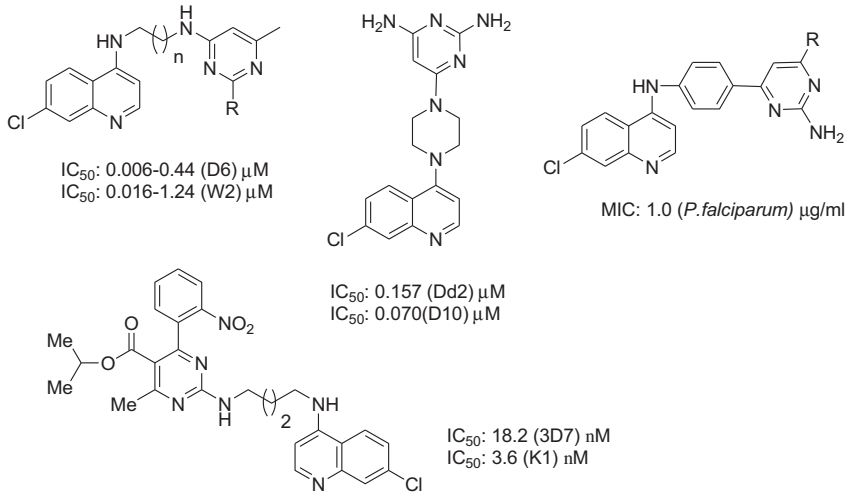


**Fig. 3.** Quinoline–pyrimidine and quinoline–pyrimidine carboxylate hybrids.

decrease in antimalarial activity against both the chloroquine sensitive and chloroquine resistant strains of *P. falciparum*. However, comparison of hybrids **5b**, **5c** with **6b**, **6c** having an identical butyl spacer showed that incorporation of isopropyl ester at C-5 of pyrimidine motif (**5b** and **6b)** increased the antimalarial activity against the $CQ^S$ strain whereas considerable decrease in activity was observed for $CQ^R$ strain of *P. falciparum*. Also, the most potent compound **5b** of the series displayed 2-fold increase in antimalarial activity than the standard CQ against $CQ^R$ strain of *P. falciparum*. When the diaminoalkyl linker of compound **6a** was replaced with relatively less basic alkoxy amino linker **5d** considerable decrease in antimalarial activity was observed which in turn linked to the decreased accumulation of compound *via* pH trapping into the digestive vacuole. It was not unexpected since the basicity of alkyl chain linker plays crucial role in determining the antimalarial activity of this class of compounds. Furthermore, the introduction of a nitro substituent on the phenyl ring at the C-4 position of the pyrimidine core to create **5c** resulted in a significant increase in antiplasmodial activity in comparison to the p-chloro/p-fluoro substituents (**5e** and **5f**). Moreover, the hybrid **5g** lacking a C-4 substituent on the pyrimidine motif led to an increase in antimalarial activity against both the $CQ^S$ as well as $CQ^R$ strains of *P. falciparum*. However, although the antimalarial activity of **5g** was superior to **5c**, **5e** & **5f**, it was less than the corresponding C-4 phenyl substituted analogs **5b** as well as **6b**.

Thus, the SAR study suggested that both the substitution of the C-4 phenyl group with electron withdrawing groups and alterations in basicity of linker leads to better antimalarial activity. Unfortunately, these compounds suffer from high ClogP values which are in the range 5–8 (Table 1), which are suggestive of the fact that these possess limited aqueous solubility. However, it is not a serious limitation in view of recent advancements in formulation methods.

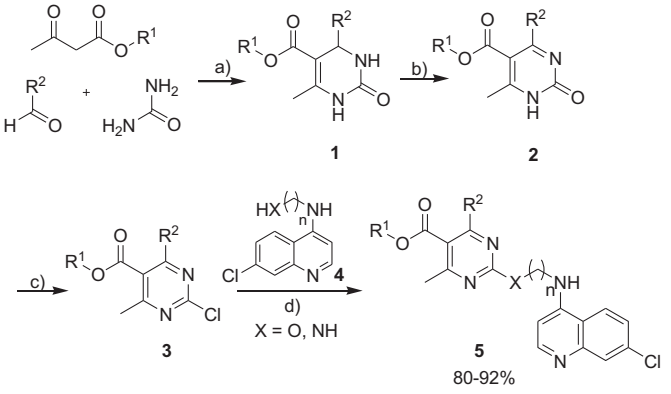


**Scheme 1.** Reagents and conditions. (a) $NH_4Cl$, 100 °C, 3 h, (b) 60% $HNO_3$, 0 °C, 30 min, (c) $POCl_3$, 105 °C, 45 min, (d) THF/MeCN, $K_2CO_3$, 70 °C, 48 h.

### 3.2. Cytotoxicity and antiviral activity

Compounds **5a**–**g** were evaluated for their toxicity against various (HeLa, Vero, CRFK, HEL and MDCK) cell cultures (Table 1 & SI Table S1). Toxicity data revealed that these compounds exhibit high toxicity (low $CC_{50}$) against MDCK cell cultures while $CC_{50}$ values are quiet high for other cell cultures. The $CC_{50}$ values for inhibition of MDCK cells summarized in Table 1 indicate that the strongest antimalarial compound **5b** was mildly cytotoxic (Table 1). Further, the ratio of the cytotoxicity ($CC_{50}$ in μM) and *in vitro* antimalarial activity ($IC_{50}$ in nM for Dd2 strain) enabled the determination of selectivity index (SI) for these compounds. Compound **5d** with alkoxy amino linker and compound **5g** bearing C-4 unsubstituted pyrimidine motif exhibited high $CC_{50}$ values and thus led to fairly safe selectivity index values (Table 1). Compound **5d** having less basic alkyl spacer, displayed highest SI (43.6) whereas the most potent compound **5b** exhibit relatively low SI value (3.92). Thus, the compounds depicted structure dependent SI values.

Chloroquine is known to elicit antiviral effects against several viruses, including human immunodeficiency virus type 1, HCoV-229E, hepatitis B virus, and herpes simplex virus type 1 [34–37]. Thus, we determined *in vitro* antiviral activities of **5a**–**g** against (i) herpes simplex virus-1 (HSV-1; KOS), herpes simplex virus-2 (HSV-2; G), vaccinia virus, vesicular stomatitis virus, herpes simplex virus-1 (TK-KOS ACVR) in HEL cell cultures, (ii) parainfluenza-3 virus, reovirus-1, Sindbis virus, Coxsackie virus B4, Punta Toro virus in vero cell cultures, (iii) influenza A virus (H1N1 and H3N2) and influenza B virus in MDCK cell cultures, (iv) vesicular stomatitis virus, coxsackie virus B4, respiratory syncytial virus in HeLa cell cultures, (v) cytomegalovirus using AD-169 and Davis strain in HeL cells, (vi) varicella-zoster virus (VZV) in HEL cells (SI Table S1) and (vii) feline corona virus (FIPV) and feline herpes virus activity in CRFK cell cultures (Table 2). The anti-viral activity of most of the compounds was not impressive except compounds **5a** and **5c** which exhibited relatively low $EC_{50}$'s only against the feline corona virus (FIPV) and feline herpes virus in CRFK cell cultures (Table 2).

**Table 1**
*In vitro* antimalarial activity of compounds **5a–g** against *P. falciparum* ($CQ^S$) D10 strain and ($CQ^R$) Dd2 strain for $n = 3$ ($n$ = number of replicates).

| Compound | Structure | Yield (%) | D10 $IC_{50}$ (nM)[a,b] | Dd2 $IC_{50}$ (nM)[b,c] | *C* log *P*[d] | $CC_{50}$ (μM)[e,f] | SI[g] |
|---|---|---|---|---|---|---|---|
| **5a** | 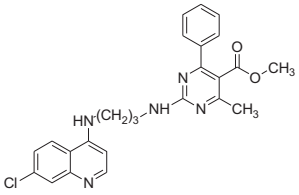 | 86 | 659 | 542 | 6.71 | 1.7 | 3.13 |
| **5b** | 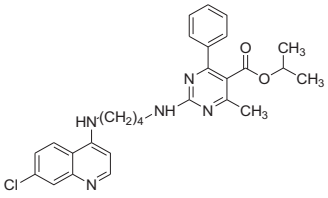 | 83 | 156 | 153 | 7.66 | 0.6 | 3.92 |
| **5c** | 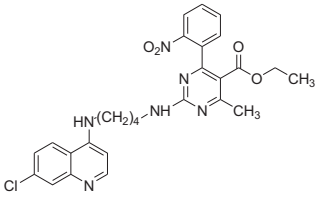 | 75 | 1461 | nd | 7.10 | 0.8 | – |
| **5d** | 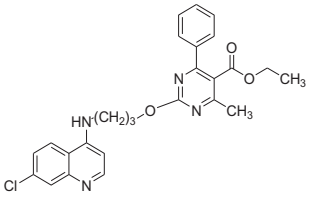 | 90 | 478 | 483 | 7.24 | 21.1 | 43.6 |
| **5e** | 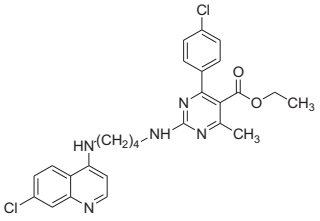 | 85 | 1926 | nd | 8.07 | 2.2 | – |
| **5f** | 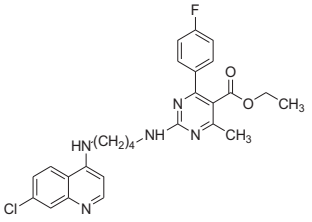 | 72 | 2759 | nd | 7.50 | 11.4 | – |
| **5g** | 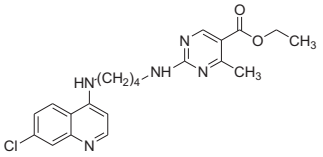 | 89[h] | 211 | 336 | 5.25 | 10.3 | 30.65 |
| **6a**[i] | 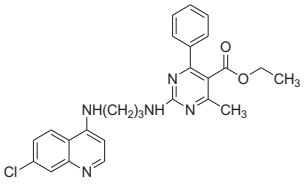 | – | 202[j] | 26.1[k] | 6.82 | 0.8 | 15.33 |

(*continued on next page*)

**Table 1** (*continued*)

| Compound | Structure | Yield (%) | D10 $IC_{50}$ (nM)[a,b] | Dd2 $IC_{50}$ (nM)[b,c] | *C* log *P*[d] | $CC_{50}$ (μM)[e,f] | SI[g] |
|---|---|---|---|---|---|---|---|
| **6b**[i] | 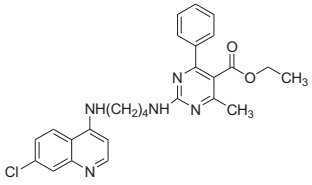 | – | 247.5[j] | 52.2[k] | 7.35 | 0.9 | 34.41 |
| **6c**[i] | 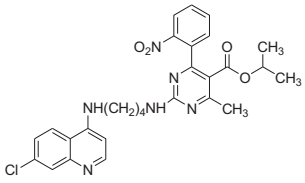 | – | 18.2[j] | 3.6[k] | 7.3 | 2.3 | 638 |
| CQ | | | 35 | 221.9 | – | – | – |
| ASN | | | – | 31.2 | – | – | – |
| MMV390048 | | | – | 17.8 | | | |

[a] CQ sensitive strain.
[b] Data represents the mean of three independent experiments.
[c] CQ resistant strain.
[d] Calculated from Chem draw Ultra 11.0.
[e] Determined on Madin Darby canine kidney (MDCK) cells.
[f] 50% cytotoxic concentration, as determined by measuring the cell viability with the colorimetric formazan-based MTS assay (reference drugs used: Oseltamivir carboxylate $CC_{50}$/MIC > 100, Ribavirin $CC_{50}$/MIC > 100, Amantadine $CC_{50}$/MIC > 200 and Rimantadine $CC_{50}$/MIC > 200).
[g] Selectivity index (S.I.) is calculated as $CC_{50}/IC_{50}$ (Dd2 Strain) ratio.
[h] Prepared by using perhydro 1,3-oxazine (1.5 equiv.) as formaldehyde equivalent ($CH_3CN$:TFA (10:1, v/v) solution/70 °C) [31].
[i] See Ref. [29].
[j] 3D7 strain used.
[k] K1 strain used.

### 3.3. Mode of action studies

#### 3.3.1. Heme binding studies

Quinoline antimalarials (e.g., CQ, amodiaquine and quinine) act principally by forming adducts with ferriprotoporphyrin IX, thus blocking haemozoin formation [38]. In this study, we have evaluated the mechanism of antimalarial activity of the most potent compound **5b** of the series by studying its binding with heme [Fe(III)PPIX] in solution and inhibition of β-hematin formation using UV–visible spectrophotometer. The incremental addition of **5b** (0–25 μM) into monomeric heme (2.4 μM, DMSO:$H_2O$/4:6, *v*/*v*) in 0.02 M HEPES buffer (pH 7.4) showed a substantial decrease in the intensity of the Fe(III) PPIX Soret band at 402 nm with no shift in the wavelength of the absorption maximum (Fig. 4). The titration of monomeric heme was also performed at the *Plasmodial* food vacuole pH 5.6 using MES buffer instead of HEPES to ensure that the compound **5b** binds with heme even at acidic pH (S1). A 1:1 stoichiometry of the most stable complex of **5b** with monomeric heme at pH 7.4 and 5.6 was established from the Job's plot (SI Figure S1). The association constants (Table 3) were calculated by analyzing the titration curves obtained at pH 7.4 using HypSpec—a non-linear least square fitting programme [39]. The binding of CQ with heme under identical conditions was also determined in the similar manner and the results are presented in Table 3 for comparison. Table 3 shows that the association constants for the complexes formed between monomeric heme and **5b** (log *K* 4.96) are comparable with those of standard antimalarial drug, CQ (log *K* 5.15). Furthermore, the decrease of apparent pH from 7.4 to 5.6 (Table 3) has little effect on the binding constants indicating binding is stronger even at acidic pH.

**Table 2**
Anti-Feline Corona Virus (FIPV) and anti-Feline Herpes Virus activity and cytotoxicity in Crandell-Rees Feline Kidney (CRFK) cell cultures.

| Compound | $CC_{50}$ (μM)[a] | $EC_{50}$ (μM)[b] | |
|---|---|---|---|
| | | Feline corona virus (FIPV) | Feline herpes virus |
| **5a** | 25.1 | 1.1 | >20 |
| **5b** | 50.6 | >20 | >20 |
| **5c** | >100 | 9.0 | >100 |
| **5d** | >100 | >100 | >100 |
| **5e** | >100 | >100 | >100 |
| **5f** | >100 | >100 | >100 |
| **5g** | >100 | >100 | >100 |
| HHA (μg/ml) | >100 | 32.5 | 2.9 |
| UDA (μg/ml) | 63.2 | 1.6 | 1.0 |
| Ganciclovir | >100 | >100 | 4.1 |

[a] 50% Cytotoxic concentration as determined by measuring the cell viability with the colorimetric formazon-based MTS assay.
[b] 50% Effective concentration or concentration producing 50% inhibition of virus-induced cytopathic effect as determined by measuring the cell viability with the colorimetric formazon-based MTS assay.

To further establish the binding of **5b** with monomeric heme, $^1$H NMR titrations were performed and shifts in the peaks as well as peak intensity noted. The addition of 30 mol% of heme dissolved in 40% DMSO to a solution of **5b** in 40% DMSO:$D_2O$\$D_2SO_4$ (10 μl) caused a shift in the aromatic proton signals (Fig. 5), indicating binding of **5b** with heme but further addition of heme led to broadening of the peaks. An equimolar (3.9 μmol) solution of hemin chloride and **5b** when analyzed in mass spectrometer depicted an intense molecular ion peak at 1119.3769 Da (Fig. 6a), corresponding to the molecular formula $C_{62}H_{62}ClFeN_9O_6$, suggesting the formation of 1:1 complex. Thus, we propose that **5b** interacts with heme by replacing chloride atom of hemin chloride and coordinating the iron atom with its endocyclic quinoline nitrogen as proposed in Fig. 6b.

Similar titration of dimers of μ-oxo type (10 μM) at pH 5.8 using standard procedure [29] with increasing concentration of

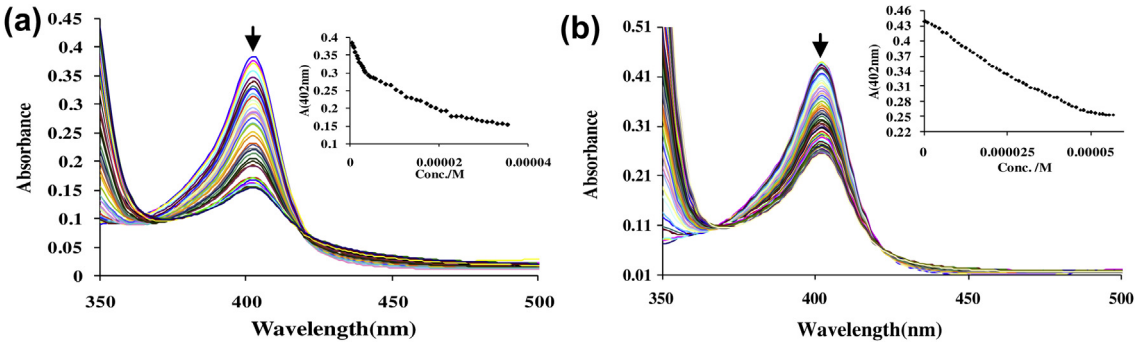


**Fig. 4.** Titration of **5b** with monomeric heme at (a) pH 7.4, (b) pH 5.6.

compound **5b** (0–14 μM), resulted in decrease in intensity of broad peak at 362 nm (Fig. 7a, S1). Further, Job's plot calculations indicated a 1:1 stoichiometry for the most stable μ-oxo: **5b** complex (Fig. 7b). In Table 3 the association constants of **5b** (log *K* 5.72) are compared to that of standard CQ (log *K* 5.58) and also suggests that the binding of **5b** is stronger with μ-oxo heme (log *K* 5.72) than monomeric heme (log *K* 4.96). Thus, the compound **5b** inhibits hemozoin formation by blocking the growing face of heme resulting in the observed antimalarial activity. Furthermore, the β-hematin inhibition assay (SI Table S2) shows that there is no correlation between antimalarial activity and β-hematin inhibition and also, all the compounds inhibit β-hematin formation although less than that of standard CQ.

### 3.3.2. *DNA binding studies*

The mechanism of many antimalarial drugs such as CQ, quinacrine and quinine relies upon the interaction with DNA presumably through ionic interactions between phosphate groups of DNA and protonated amine in addition to the interactions between aromatic nuclei of the drug with nucleotide bases [40,41]. Therefore, the DNA binding properties of 4-aminoquinoline–pyrimidine hybrids have been evaluated using both the UV–visible spectrophotometer and fluorescence spectrophotometry in order to probe interaction of these compounds with DNA. The addition of CT-DNA (4–200 μM) to the buffered methanolic solution of **5b** (30 μM) induced hyperchromic shift of 112% in absorption band at 255 nm whereas hypochromic shift of 37% in the characteristic quinoline ring absorption at 330 nm (Fig. 8). Also, the bathochromic shift of ~3 nm was observed for both the absorptions. The observed hyperchromic as well as hypochromic shifts in absorption bands of **5b** upon addition of DNA results from the intercalation of **5b** with CT DNA as suggested in the literature [42]. The intercalative nature of interaction of compound **5b** with CT DNA was additionally supported by thermal denaturation experiment. Intercalation of molecules into the double helix is known to stabilize the DNA against thermal strand separation and thus increases thermal melting temperature ($T_m$) [43,44]. The derivative melting curve presented in Fig. 9 shows an increase of 7.5 °C in thermal melting temperature of CT DNA upon addition of **5b** which is less than that observed for the CQ (Table S3). Thus, both the UV–visible titrations and thermal denaturation experiment advocate partial intercalative nature of interactions between compound **5b** and CT DNA.

Further, to visualize the effect of DNA base composition, the fluorescence titrations of **5b** were performed with both GC-rich CT DNA and AT-rich pUC18 DNA in buffered methanol. Fig. 10 shows decrease in the intensity of the emission band of **5b** at 380 nm, upon addition of increasing concentration of both the DNAs. A shift of 80 nm in emission band at 380 nm was observed upon addition of CT DNA but no such shift in emission band was observed for pUC18 DNA. Comparison of binding constant of **5b** with CT DNA (log *K* 5.76) and pUC18 DNA (log *K* 5.73) calculated from titration data using HypSpec [39], suggest that **5b** does not discriminate between GC rich DNA and AT rich DNA.

**Table 3**
Binding constant (log *K*) of **5b** and CQ with heme and DNA.

| Compound | Monomeric heme, log $K \pm \sigma$ | | μ-oxoheme, log $K \pm \sigma$ | CT DNA, log *K* | pUC18 DNA, log *K* |
|---|---|---|---|---|---|
| | pH 5.6 | pH 7.4 | pH 5.8 | | |
| **5b**[a] | 4.58 ± 0.042 | 4.96 ± 0.029 | 5.72 ± 0.025 | 5.76 | 5.73 |
| CQ | 4.65 ± 0.052 | 5.15 ± 0.176 | 5.58 ± 0.006 | nd | nd |
| Stoichiometry | 1:1 | | 1:1 | nd | |

[a] Calculated from HypSpec software.

## 4. Conclusions

A series of potent 4-aminoquinoline–pyrimidine hybrids with antimalarial activity in nanomolar range were reported. The compound **5b** exhibits lowest $IC_{50}$ value within the series against both $CQ^S$ and $CQ^R$ strains of *P. falciparum*. These hybrids displayed mild toxicity against MDCK cell cultures. The antiviral activity profiles of these hybrids indicate that the compound **5a** and **5c** effectively inhibit feline corona virus and feline herpes virus. Further, the mechanism of observed antimalarial activity was established in terms of binding with heme as well as DNA.

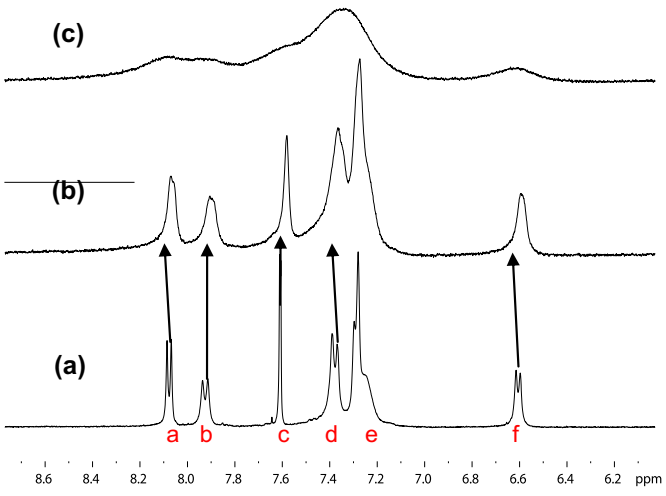


**Fig. 5.** The 400 MHz $^1$H spectra of **5b** upon addition of heme (a) 0 mol%, (b) 30 mol%, (c) 50 mol% (in 40% DMSO:$D_2O$\$D_2SO_4$ (10 μl)) [$\Delta\delta$ for peak: a = 0.002, b = 0.013, c = 0.023, d = 0.008, e = 0.007, f = 0.007].

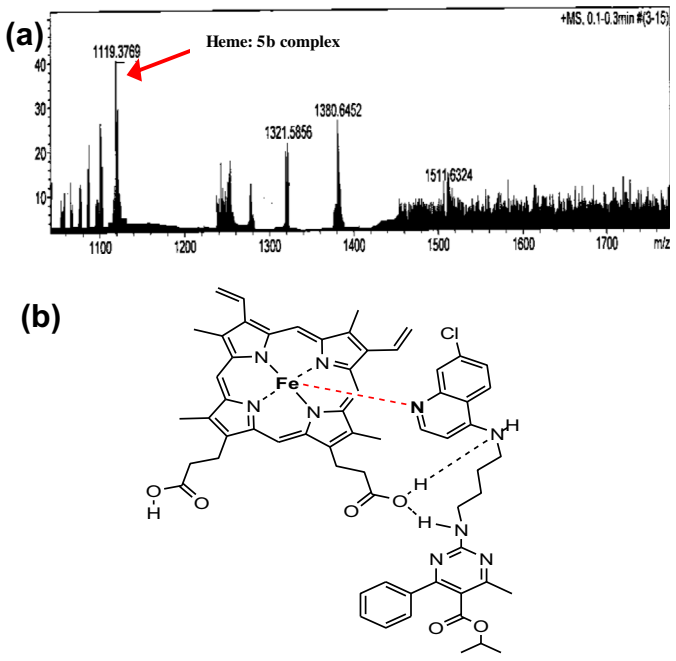


**Fig. 6.** (a) The solution phase mass spectra of **5b** (3.9 μmoles) upon addition of monomeric heme (3.9 μmoles) in 40% DMSO, (b) proposed binding of heme with **5b** (for optimized structure of **5b**, see Figure S2).

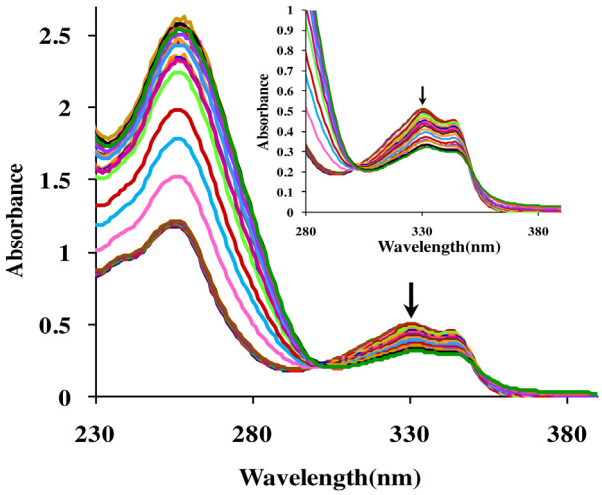


**Fig. 8.** Absorption spectra of **5b** (30 μM) in the presence of increasing CT DNA concentration (4–200 μM); inset shows zoom between 280 and 390 nm.

## 5. Experimental

### 5.1. General

All liquid reagents were dried/purified following recommended drying agents and/or distilled over 4 Å molecular sieves. THF was dried (Na-benzophenone ketyl) under nitrogen. $^1$H NMR (300 MHz) and $^{13}$C (75 MHz) NMR spectra were recorded in $CDCl_3$ on a multinuclear Jeol FT-AL-300 spectrometer with chemical shifts being reported in parts per million ($\delta$) relative to internal tetramethylsilane (TMS, $\delta$ 0.0, $^1$H NMR) or chloroform ($CDCl_3$, $\delta$77.0, $^{13}$C NMR). Mass spectra were recorded at Department of Chemistry, Guru Nanak Dev University, Amritsar on a Bruker LC-MS MICROTOF II spectrometer. Elemental analysis was performed on FLASH EA 112 (Thermo electron Corporation) analyzer at Department of Chemistry, Guru Nanak Dev University, Amritsar and the results are quoted in %. IR spectra were recorded on Perkin Elmer FTIR-C92035 Fourier transform spectrometer in the range 400–4000 cm$^{-1}$ using KBr pellets. Melting points were determined in open capillaries and are uncorrected. For monitoring the progress of a reaction and for comparison purpose, thin layer chromatography (TLC) was performed on pre-coated aluminum sheets of Merck ($60F_{254}$, 0.2 mm) using an appropriate solvent system. The chromatograms were visualized under UV light. For column chromatography silica gel (60–120 mesh) was employed and eluents were ethyl acetate/hexane or ethyl acetate/methanol mixtures. The steady state fluorescence experiments were carried out on Perkin Elmer LS55 fluorescence spectrometer at ambient temperature. UV–visible spectral studies were conducted on Shimadzu 1601 PC spectrophotometer with a quartz cuvette (path length, 1 cm). The absorption spectra have been recorded between 1100 and 200 nm. The cell holder of the spectrophotometer was thermostated at 25 °C for consistency in the recordings.

### 5.2. General procedure for synthesis of *5a* and *5b*

To the stirred solution of **3** (2 mmol) and potassium carbonate (5 mmol) in dry THF (30 ml), a solution of appropriate 4-aminoquinoline **4** (1.0 mmol) in dry THF (50 ml) was added. The reaction mixture was stirred for 48 h at room temperature. The reaction mixture was filtered and THF was removed under vacuum. The residue was purified by column chromatography using MeOH/ethyl acetate as eluent to obtain corresponding **5**, which was recrystallized from DCM/hexane. Using this procedure the following compounds were isolated.

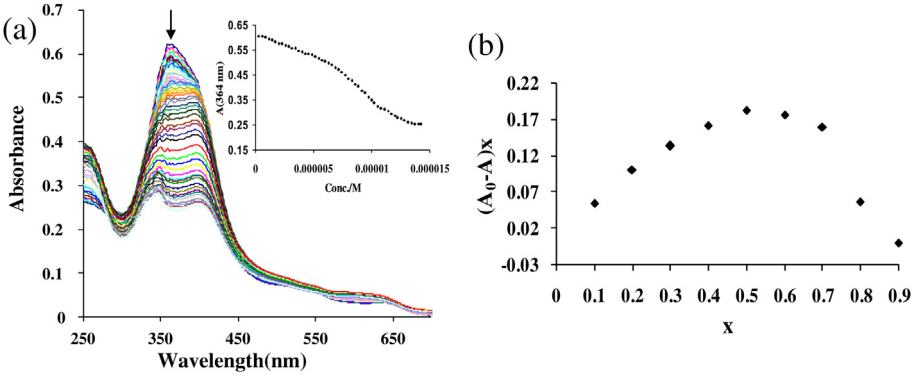


**Fig. 7.** (a) Titration of **5b** with μ-oxo heme at pH 5.8, (b) Job plot of μ-oxo heme complex formation at pH 5.8. $x$ = [**5b**]/[**5b**] + [heme] is the mole fraction of the **5b**, $A_0$ is the absorbance, when $x = 1$ and $A$ is the absorbance at respective values of $x$.

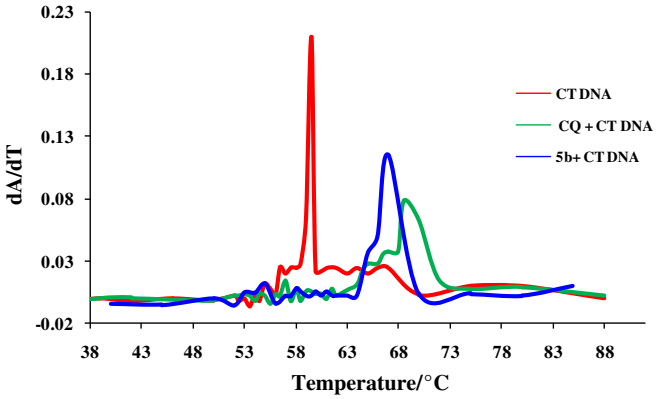


**Fig. 9.** Derivative melting curves of CT DNA, **5b** + CT DNA and **CQ** + CT DNA.

*5.2.1. Methyl 2-(3-((7-chloroquinolin-4-yl)amino)propylamino)-4-methyl-6-phenylpyrimidine-5-carboxylate (**5a**)*

White solid. Rf: 0.47 (4% MeOH/ethyl acetate). Yield: 86%. m.p.105 °C. IR (KBr): $\nu_{max}$ 770, 1267, 1709, 2928, 3427 $cm^{-1}$. $^1H$ NMR (300 MHz, $CDCl_3$, 25 °C): $\delta$ 2.00 (q, $J$ = 6.3 Hz, 2H, $CH_2$), 2.49 (s, 3H, C6-$CH_3$), 3.46 (m, 2H, $CH_2$), 3.58 (s, 3H, ester-$CH_3$), 3.68 (q, $J$ = 6.6 Hz, 2H, $CH_2$), 5.57 (br, 1H, NH), 6.41 (d, 1H, ArH), 6.44 (br, 1H, NH), 7.39–7.54 (m, 7H, ArH), 7.91 (s, 1H, ArH), 8.48 (d, 1H, ArH). $^{13}C$ NMR (75 MHz, $CDCl_3$, 25 °C): $\delta$ 14.8, 20.6, 30.0, 31.6, 43.8, 90.6, 92.3, 112.7, 116.8, 119.5, 120.2, 121.5, 126.5, 141.3, 143.6, 153.5, 159.1, 160.8. Anal. Calcd. for $C_{25}H_{24}N_5O_2Cl$: C, 65.00; H, 5.24; N, 15.10; Found: C, 65.14; H, 5.19; N, 14.99. MS: $m/z$ 462 [$M^+$].

*5.2.2. i-Propyl 2-(4-((7-chloroquinolin-4-yl)amino)butylamino)-4-methyl-6-phenylpyrimidine-5-carboxylate (**5b**)*

White solid. Rf: 0.41 (4% MeOH/ethyl acetate). Yield: 83%. m.p. 140 °C. IR (KBr): $\nu_{max}$ 1368, 1724, 2993, 3473 $cm^{-1}$. $^1H$ NMR (400 MHz, $CDCl_3$, 25 °C): $\delta$ 1.0 (d, $J$ = 5.6 Hz, 6H, 2 × ester-$CH_3$), 1.78 (m, 4H, $CH_2$), 2.46 (s, 3H, C6-$CH_3$), 3.33 (m, 2H, $CH_2$), 3.50 (m, 2H, $CH_2$), 4.99 (m, 1H, ester-CH), 5.44 (br, 1H, NH), 5.67 (br, 1H, NH), 6.34 (d, $J$ = 5.3 Hz, 1H, ArH), 7.27–7.63 (m, 7H, ArH), 7.93 (d, $J$ = 1.4 Hz, 1H, ArH), 8.46 (d, $J$ = 5.3 Hz, 1H, ArH). $^{13}C$ NMR (75 MHz, $CDCl_3$, 25 °C): $\delta$ 21.3, 22.9, 25.8, 27.4, 40.7, 42.9, 68.9, 98.9, 116.0, 117.0, 121.3, 125.3, 129.5, 135.0, 138.9, 148.4, 150.0, 151.3, 161.2, 165.8, 166.9, 168.3. Anal. Calcd. for $C_{28}H_{30}N_5O_2Cl$: C, 66.72; H, 6.00; N, 13.89; Found: C, 66.50; H, 5.88; N, 13.65. MS: $m/z$ 503.2 [$M^+$].

*5.3. General procedure for the synthesis of compound **5c–g***

To the stirred solution of appropriate 4-aminoquinoline **4** in dry acetonitrile (50 ml) mixture of **3** (in a 1:2 molar ratio) and potassium carbonate in dry acetonitrile was added. The reaction mixture was refluxed for 24 h and then filtered. Acetonitrile was removed under vacuum and the residue was purified by column chromatography using MeOH/ethyl acetate as eluent to give **5** which is recrystallized from DCM/hexane.

*5.3.1. Ethyl 2-(4-((7-chloroquinolin-4-yl)amino)butylamino)-4-methyl-6-(2-nitrophenyl)pyrimidine-5-carboxylate (**5c**)*

Yellow solid. Rf: 0.28 (4% MeOH/ethyl acetate). Yield: 75%. m.p. 72 °C. IR (KBr): $\nu_{max}$ 769, 1550, 1355, 1720, 2930, 3365 $cm^{-1}$. $^1H$ NMR (400 MHz, $CDCl_3$, 25 °C): $\delta$ 0.87 (t, $J$ = 7.1 Hz, 3H, ester-$CH_3$), 1.76 (m, 4H, $CH_2$), 2.57 (s, 3H, C6-$CH_3$), 3.27 (m, 2H, $CH_2$), 3.47 (m, 2H, $CH_2$), 3.96 (q, $J$ = 7.0 Hz, 2H, ester-$CH_2$), 6.07 (br, 1H, NH), 6.26 (d, $J$ = 4.8 Hz, 1H, ArH), 6.33 (br, 1H, NH), 7.22–7.86 (m, 6H, ArH), 8.11 (s, 1H, ArH), 8.32 (d, $J$ = 5.4 Hz, 1H, ArH). $^{13}C$ NMR (100 MHz, $CDCl_3$, 25 °C): $\delta$ 12.5, 22.1, 24.4, 28.6, 39.7, 42.2, 59.7, 97.4, 115.6, 121.3, 123.2, 124.5, 125.0, 128.2, 128.6, 131.9, 134.7, 145.2, 148.3, 150.1, 159.9, 165.3, 176.3. Anal. Calcd. for $C_{27}H_{27}N_6O_4Cl$: C, 60.62; H, 5.09; N, 15.7; Found: C, 60.34; H, 5.01; N, 15.58. MS: $m/z$ 534.2 [$M^+$].

*5.3.2. Ethyl 2-(3-((7-chloroquinolin-4-yl)amino)propoxy)-4-methyl-6-phenylpyrimidine-5-carboxylate (**5d**)*

White solid. Rf: 0.38 (4% MeOH/ethyl acetate). Yield: 90%. m.p.110 °C. IR (KBr): $\nu_{max}$ 1255, 1775, 2969, 3530 $cm^{-1}$. $^1H$ NMR (300 MHz, $CDCl_3$, 25 °C): $\delta$ 1.05 (t, $J$ = 7.2 Hz, 3H, ester-$CH_3$), 2.43 (m, 2H, $CH_2$), 2.59 (s, 3H, C6-$CH_3$), 3.56 (m, 2H, $CH_2$), 4.13 (t, $J$ = 7.2 Hz, 2H, $CH_2$), 4.68 (q, $J$ = 6.0 Hz, 2H, ester-$CH_2$), 5.70 (br, 1H, NH), 6.41 (d, $J$ = 5.4 Hz, 1H, ArH), 7.20–7.76 (m, 7H, ArH), 7.93 (d, $J$ = 2.1 Hz, 1H, ArH), 8.49 (d, $J$ = 5.4 Hz, 1H, ArH). $^{13}C$ NMR (75 MHz, $CDCl_3$, 25 °C): $\delta$ = 13.5, 22.8, 27.7, 41.2, 61.7, 66.4, 121.3, 125.3, 130.2, 151.9. Anal. Calcd. for $C_{26}H_{25}N_4O_3Cl$: C, 65.47; H, 5.28; N, 11.75; Found: C, 65.12; H, 4.99; N, 11.89. MS: $m/z$ 476.1 [$M^+$].

*5.3.3. Ethyl 4-(4-chlorophenyl)-2-(4-((7-chloroquinolin-4-yl)amino)butylamino)-6-methylpyrimidine-5-carboxylate (**5e**)*

Yellow solid. Rf: 0.54 (4% MeOH/ethyl acetate). Yield: 85%. m.p. 135 °C. IR (KBr): $\nu_{max}$ 1065, 1720, 2930, 3489 $cm^{-1}$. $^1H$ NMR (300 MHz, $CDCl_3$, 25 °C): $\delta$ 1.03 (t, $J$ = 6.9 Hz, 3H, ester-$CH_3$), 1.86 (m, 4H, $CH_2$), 2.46 (s, 3H, C6-$CH_3$), 3.40 (m, 2H, $CH_2$), 3.59 (m, 2H, $CH_2$), 4.07 (q, $J$ = 6.0 Hz, 2H, ester-$CH_2$), 5.50 (br, 1H, NH), 5.78 (br, 1H, NH), 6.36 (d, $J$ = 5.7 Hz, 1H, ArH), 7.25–7.37 (m, 5H, ArH), 7.48 (d,

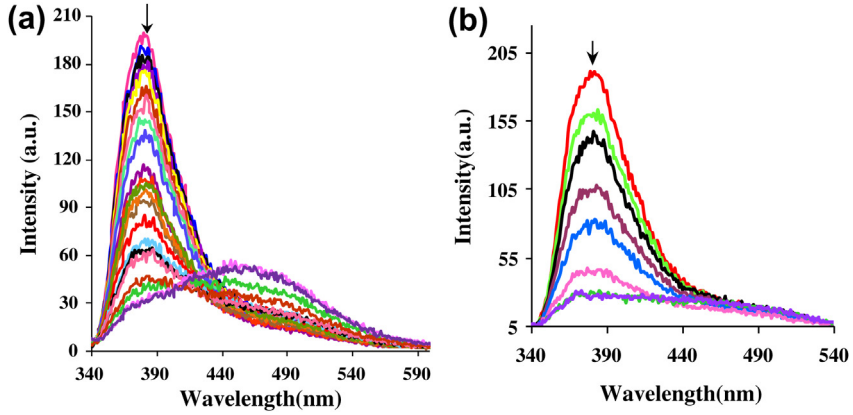


**Fig. 10.** Fluorescence emission spectra ($\lambda_{ex}$ = 330 nm, $\lambda_{em}$ = 376 nm) of **5b** (17.1 μM) in buffered $CH_3OH$ upon addition of increasing concentrations of (a) CT DNA (0.5–150 μM), (b) pUC18 DNA (0.02–15 μM).

$J$ = 8.4 Hz, 1H, ArH), 7.96 (d, $J$ = 7.8 Hz, 1H, ArH), 8.42 (d, $J$ = 5.7 Hz, 1H, ArH). $^{13}$C NMR (75 MHz, $CDCl_3$, 25 °C): $\delta$ 16.5, 28.8, 30.2, 32.5, 64.1, 101.8, 128.3, 131.3, 132.2, 143.2, 152.4, 161.6, 167.7. Anal. Calcd. for $C_{27}H_{27}N_5O_2Cl_2$: C, 61.84; H, 5.19; N, 13.35; Found: C, 61.57; H, 5.05; N, 13.12. MS: $m/z$ 523.1 [$M^+$].

#### 5.3.4. Ethyl 4-(4-fluorophenyl)-2-(4-((7-chloroquinolin-4-yl) amino)butylamino)-6-methylpyrimidine-5-carboxylate (**5f**)

Yellow solid. Rf: 0.34 (4% MeOH/ethyl acetate). Yield: 72%. m.p. 112 °C. IR (KBr): $\nu_{max}$ 1156, 1682, 1333, 2928, 3395 cm$^{-1}$. $^1$H NMR (300 MHz, $CDCl_3$, 25 °C): $\delta$ 1.02 (t, $J$ = 7.2 Hz, 3H, ester-$CH_3$), 1.83 (m, 4H, $CH_2$), 2.46 (s, 3H, C6-$CH_3$), 3.38 (m, 2H, $CH_2$), 3.49 (m, 2H, $CH_2$), 4.08 (q, $J$ = 6.0 Hz, 2H, ester-$CH_2$), 5.40 (br, 1H, NH), 5.74 (br, 1H, NH), 6.37 (d, $J$ = 5.4 Hz, 1H, ArH), 7.04–7.55 (m, 6H, ArH), 7.95 (d, $J$ = 2.1 Hz, 1H, ArH), 8.47 (d, $J$ = 5.7 Hz, 1H, ArH). $^{13}$C NMR (75 MHz, $CDCl_3$, 25 °C): $\delta$ 18.5, 29.6, 31.2, 63.5, 99.8, 126.3, 133.3, 145.2, 153.4, 160.4, 171.7. Anal. Calcd. for $C_{27}H_{27}N_5O_2ClF$: C, 63.84; H, 5.36; N, 13.79; Found: C, 63.76; H, 5.23; N, 13.88. MS: $m/z$ 507.1 [$M^+$].

#### 5.3.5. Ethyl 2-(3-((7-chloroquinolin-4-yl)amino)propylamino)-4-methylpyrimidine-5-carboxylate (**5g**)

White solid. Rf: 0.38 (4% MeOH/ethyl acetate). Yield: 89%. m.p. 143 °C. IR (KBr): $\nu_{max}$ 1097, 1702, 2973, 3365 cm$^{-1}$. $^1$H NMR (300 MHz, $CDCl_3$, 25 °C): $\delta$ 1.36 (t, $J$ = 7.1 Hz, 3H, ester-$CH_3$), 1.84 (m, 4H, $CH_2$), 2.64 (s, 3H, C6-$CH_3$), 3.40 (d, $J$ = 5.4 Hz, 2H, $CH_2$), 3.58 (m, 2H, $CH_2$), 4.31 (q, $J$ = 7.2 Hz, 2H, ester-$CH_2$), 5.68 (br, 2H, NH), 6.40 (d, $J$ = 5.7 Hz, 1H, ArH), 7.33 (d, $J$ = 2.1 Hz, 1H, ArH), 7.84 (d, $J$ = 6.0 Hz, 1H, ArH), 7.95 (d, $J$ = 2.1 Hz, 1H, ArH), 8.45 (d, $J$ = 6.0 Hz, 1H, ArH), 8.70 (s, 1H, ArH). $^{13}$C NMR (75 MHz, $CDCl_3$, 25 °C): $\delta$ 14.3, 40.8, 60.5, 99.1, 125.3, 128.8, 149.0, 151.9. Anal. Calcd. for $C_{21}H_{24}N_5O_2Cl$: C, 60.94; H, 5.84; N, 16.92; Found: C, 61.10; H, 5.75; N, 16.79. MS: $m/z$ 413.1 [$M^+$].

## 6. Material and methods

### 6.1. In vitro antimalarial activity assay

The test samples were tested in triplicate on one or two separate occasions against chloroquine sensitive ($CQ^S$) strain of *P. falciparum* (D10). Continuous *in vitro* cultures of asexual erythrocyte stages of *P. falciparum* were maintained using a modified method of Trager and Jensen [45]. Quantitative assessment of antiplasmodial activity *in vitro* was determined *via* the parasite lactate dehydrogenase assay using a modified method described by Makler et al. [46]. The test samples were prepared to a 20 mg/ml stock solution in 100% DMSO and sonicated to enhance solubility. Samples were tested as a suspension if not completely dissolved. Stock solutions were stored at −20 °C. Further dilutions were prepared on the day of the experiment. Chloroquine (CQ) was used as the reference drug in all experiments. Test samples were initially tested at three concentrations (10 μg/ml, 5 μg/ml and 2.5 μg/ml) to determine the starting concentration for the full dose–response assay. CQ was tested at three concentrations namely 30 ng/ml, 15 ng/ml and 7.5 ng/ml. A full dose–response was performed for all compounds to determine the concentration inhibiting 50% of parasite growth ($IC_{50}$-value). Test samples were tested at a starting concentration of 10 μg/ml, which was then serially diluted 2-fold in complete medium to give 10 concentrations; with the lowest concentration being 0.02 μg/ml. The same dilution technique was used for all samples. CQ was tested at a starting concentration of 1000 ng/ml. Several compounds were tested at a starting concentration of 1000 ng/ml. The highest concentration of solvent to which the parasites were exposed to had no measurable effect on the parasite viability (data not shown). The $IC_{50}$-values were obtained using a non-linear dose–response curve fitting analysis *via* Graph Pad Prism v.4.0 software.

### 6.2. Cytotoxicity and antiviral activity assay

Cytotoxicity was determined by exposing different concentrations of samples to Vero, HEL, HeLa and MDCK cells [29]. The antiviral assays were based on inhibition of virus-induced cytopathicity in HEL [herpes simplex virus type 1 (HSV-1), HSV-2 (G), vaccinia virus, and vesicular stomatitis virus], Vero (parainfluenza-3, reovirus-1, Coxsackie B4, and Punta Toro virus), HeLa (vesicular stomatitis virus, Coxsackie virus B4, and respiratory syncytial virus) and MDCK (influenza A (H1N1; H3N2) and B virus) cell cultures. Confluent cell cultures in microtiter 96-well plates were inoculated with 100 cell culture inhibitory dose-50 ($CCID_{50}$) of virus (1 $CCID_{50}$ being the virus dose to infect 50% of the cell cultures) in the presence of varying concentrations of the test compounds. Viral cytopathicity was recorded as soon as it reached completion in the control virus-infected cell cultures that were not treated with the test compounds [29].

## Acknowledgments

We gratefully acknowledge financial assistance from CSIR, New Delhi (project 01(2364)/10/EMR-II) and UGC, New Delhi for Special Assistance Programme (SAP). H.K. thanks CSIR, New Delhi for senior research fellowship. JB thanks KU Leuven for financial support (GOA 10/14).

## Appendix A. Supplementary material

Supplementary material associated with this article can be found, in the online version, at http://dx.doi.org/10.1016/j.ejmech.2013.05.046.

## References

[1] R.G.A. Feachem, A.A. Phillips, J. Hwang, C. Cotter, B. Wielgosz, B.M. Greenwood, O. Sabot, M.H. Rodriguez, R.R. Abeyasinghe, T.A. Ghebreyesus, R.W. Snow, Shrinking the malaria map: progress and prospects, Lancet 376 (2010) 1566–1578.
[2] WHO, 2010, http://www.who.int/malaria/world_malaria_report_2010/worldmalariareport2010.pdf.
[3] F.-J. Gamo, L.M. Sanz, J. Vidal, C. Cozar, E. Alvarez, J.-L. Lavandera, D.E. Vanderwall, D.V.S. Green, V. Kumar, S. Hasan, J.R. Brown, C.E. Peishoff, L.R. Cardon, J.F.G. Bustos, Thousands of chemical starting points for antimalarial lead identification, Nature 465 (2010) 305–310.
[4] M. Dondorp, F. Nosten, P. Yi, D. Das, A.P. Phyo, J. Tarning, K.M. Lwin, F. Ariey, W. Hanpithakpong, S.J. Lee, P. Ringwald, K. Silamut, M. Imwong, K. Chotivanich, P. Lim, T. Herdman, S.S. An, S. Yeung, P. Singhasivanon, N.P.J. Day, N. Lindegardh, D. Socheat, N.J. White, Artemisinin resistance in *Plasmodium falciparum* malaria, N. Engl. J. Med. 361 (2009) 455–469.
[5] M. Schlitzer, Malaria chemotherapeutics, part I: history of antimalarial drug development, currently used therapeutics, and drugs in clinical development, ChemMedChem 2 (2007) 944–986.
[6] B. Meunier, Hybrid molecules with a dual mode of action: dream or reality? Acc. Chem. Res. 41 (2008) 69–77.
[7] F.W. Muregi, A. Ishih, Next-generation antimalarial drugs: hybrid molecules as a new strategy in drug design, Drug Dev. Res. 71 (2010) 20–32.
[8] S. Manohar, S.I. Khan, D.S. Rawat, Synthesis, antimalarial activity and cytotoxicity of 4-aminoquinoline–triazine conjugates, Bioorg. Med. Chem. Lett. 20 (2010) 322–325.
[9] S. Manohar, S.I. Khan, D.S. Rawat, Synthesis of 4-aminoquinoline-1,2,3-triazole and 4-aminoquinoline-1,2,3-triazole-1,3,5-triazine hybrids as potential antimalarial agents, Chem. Biol. Drug Des. 78 (2011) 124–136.
[10] C. Biot, G. Glorian, L.A. Maciejewski, J.S. Brocard, Synthesis and antimalarial activity in vitro and in vivo of a new ferrocene–chloroquine analogue, J. Med. Chem. 40 (1997) 3715–3718.
[11] K. Chauhan, M. Sharma, J. Saxena, S.V. Singh, P. Trivedi, K. Srivastava, S.K. Puri, J.K. Saxena, V. Chaturvedi, P.M.S. Chauhan, Synthesis and biological evaluation of a new class of 4-aminoquinoline–rhodanine hybrid as potent anti-infective agents, Eur. J. Med. Chem. 62 (2013) 693–704.
[12] V.R. Solomon, W. Haq, K. Srivastava, S.K. Puri, S.B. Katti, Synthesis and antimalarial activity of side chain modified 4-aminoquinoline derivatives, J. Med. Chem. 50 (2007) 394–398.
[13] E.M. Guantai, K. Ncokazi, T.J. Egan, J. Gut, P.J. Rosenthal, R. Bhampidipati, A. Kopinathan, P.J. Smith, K. Chibale, Enone- and chalcone–chloroquinoline hybrid

analogues: in silico guided design, synthesis, antiplasmodial activity, in vitro metabolism, and mechanistic studies, J. Med. Chem. 54 (2011) 3637–3649.
[14] O.D. Cabaret, F.B. Vical, A. Robert, B. Meunier, Preparation and antimalarial activities of trioxaquines, new modular molecules with a trioxane skeleton linked to a 4-aminoquinoline, ChemBioChem 1 (2000) 281–283.
[15] I. Chiyanzu, C. Clarkson, P.J. Smith, J. Lehman, J. Gut, P.J. Rosenthal, K. Chibale, Design, synthesis and anti-plasmodial evaluation in vitro of new 4-aminoquinoline isatin derivatives, Bioorg. Med. Chem. 13 (2005) 3249–3261.
[16] S. Manohar, U.C. Rajesh, S.I. Khan, B.L. Tekwani, D.S. Rawat, Novel 4-aminoquinoline–pyrimidine based hybrids with improved in vitro and in vivo antimalarial activity, ACS Med. Chem. Lett. 3 (2012) 555–559.
[17] S.I. Pretorius, W.J. Breytenbach, C. de Kock, P.J. Smith, D.D. N'Da, Synthesis, characterization and antimalarial activity of quinoline–pyrimidine hybrids, Bioorg. Med. Chem. 13 (2012) 3249–3261.
[18] M. Sharma, V. Chaturvedi, Y.K. Manju, S. Bhatnagar, K. Srivastava, S.K. Puri, P.M. Chauhan, Substituted quinolinyl chalcones and quinolinyl pyrimidines as a new class of anti-infective agents, Eur. J. Med. Chem. 44 (2009) 2081–2091.
[19] R. Ettari, F. Bova, M. Zappala, S. Grasso, N. Micale, Falcipain-2 inhibitors, Med. Res. Rev. 30 (2010) 136–167.
[20] M. Foley, L. Tilley, Quinoline antimalarial: mechanisms of action and resistance, Int. J. Parasitol. 27 (1997) 231–240.
[21] J.X. Kelly, M.J. Smilkstein, R. Brun, W. Sergio, A.R. Cooper, K.D. Lane, A. Janowsky, R.A. Johnson, R.A. Dodean, R. Winter, D.J. Hinrichs, M.K. Riscoe, Discovery of dual function acridones as a new antimalarial chemotype, Nature 459 (2009) 270–273.
[22] N. Hossain, J. Rozenski, E.D. Clercq, P. Herdewijn, Synthesis and antiviral activity of the alpha-analogues of 1,5-anhydrohexitol nucleosides, J. Org. Chem. 62 (1997) 2442–2447.
[23] K. Singh, K. Singh, B. Wan, S. Franzblau, K. Chibale, J. Balzarini, Facile transformation of 3,4-dihydropyrimidin-2(1H)-ones to pyrimidines in vitro evaluation as inhibitor of mycobacterium tuberculosis and modulators of cytostatic activity, Eur. J. Med. Chem. 46 (2011) 2290–2294.
[24] S. Joseph, J.M. Burke, Optimization of an anti-HIV hairpin ribozyme by in vitro selection, J. Biol. Chem. 268 (1993) 24515–24518.
[25] B.C. Bookser, B.G. Ugarkar, M.C. Matelich, R.H. Lemus, M. Allan, M. Tsuchiya, M. Nakane, A. Nagahisa, J.B. Wiesner, M.D. Erion, Adenosine kinase inhibitors. Synthesis, water solubility, and antinociceptive activity of 5-phenyl-7-(5-deoxy-beta-D-ribofuranosyl) pyrrolo[2,3-d]pyrimidines substituted at C4 with glycinamides and related compounds, J. Med. Chem. 48 (2005) 7808–7820.
[26] S.L. Hargreaves, B.L. Pilkington, S.E. Russell, P.A. Worthington, The synthesis of substituted pyridylpyrimidine fungicides using palladium catalysed cross-coupling reactions, Tetrahedron Lett. 41 (2000) 1653–1656.
[27] M.G. Carlos, R.M. John, D. Charles, Nucleoside analogues and nucleobases in cancer treatment, Lancet Oncol. 3 (2002) 415–424.
[28] D.C. Martyn, A. Nijjar, C.A. Celatka, R. Mazitschek, J.F. Cortese, E. Tyndall, H. Liu, M.M. Fitzgerald, T.J. Shea, S. Danthi, J. Clardy, Synthesis and antiplasmodial activity of novel 2,4-diaminopyrimidines, Bioorg. Med. Chem. Lett. 20 (2010) 228–231.
[29] K. Singh, H. Kaur, K. Chibale, J. Balzarini, S. Little, P.V. Bharatam, 2-Aminopyrimidine based 4-aminoquinoline anti-plasmodial agents. Synthesis, biological activity, structure–activity relationship and mode of action studies, Eur. J. Med. Chem. 52 (2012) 82–97.
[30] A. Shaabani, A. Bazgir, F. Teimouri, Ammonium chloride-catalyzed one-pot synthesis of 3,4-dihydropyrimidin-2-(1*H*)-ones under solvent-free conditions, Tetrahedron Lett. 44 (2003) 857–859.
[31] K. Singh, J. Singh, P.K. Deb, H. Singh, An expedient protocol of the Biginelli dihydropyrimidine synthesis using carbonyl equivalents, Tetrahedron 55 (1999) 12873–12880.
[32] A. Puchala, F. Belaj, J. Bergman, C.O. Kappe, On the reaction of 3,4-dihydropyrimidones with nitric acid. Preparation and X-ray structure analysis of a stable nitrolic acid, J. Heterocycl. Chem. 38 (2001) 1345–1352.
[33] J.K. Natarajan, J.N. Alumasa, K. Yearick, K.A. Ekoue-Kovi, L.B. Casabianca, A.C. de Dios, C. Wolf, P.D. Roepe, 4-N-, 4-S-, and 4-O-Chloroquine analogues: influence of side chain length and quinolyl nitrogen $pK_a$ on activity vs chloroquine resistant malaria, J. Med. Chem. 51 (2008) 3466–3479.
[34] E.A. Kouroumalis, J. Koskinas, Treatment of chronic active hepatitis B (CAH B) with chloroquine: a preliminary report, Ann. Acad. Med. 15 (1986) 149–152.
[35] M.K. Kono, A.M. Tatsumi, K. Imai, T. Saito, Kuriyama, H. Shirasawa, Inhibition of human coronavirus 229E infection in human epithelial lung cells (L132) by chloroquine: involvement of p38 MAPK and ERK, Antiviral Res. 77 (2008) 150–152.
[36] W.P. Tsai, P.L. Nara, H.F. Kung, S. Oroszlan, Inhibition of human immunodeficiency virus infectivity by chloroquine, AIDS Res. Hum. Retroviruses 6 (1990) 481–489.
[37] A.K. Singh, G.S. Sidhu, R.M. Friedman, R.K. Maheshwari, Mechanism of enhancement of the antiviral action of interferon against herpes simplex virus-1 by chloroquine, J. Interferon Cytokine Res. 16 (1996) 725–731.
[38] A. Dorn, R. Stoffel, H. Matile, A. Bubendorf, R. Ridley, Malarial haemozoin/beta-haematin supports haem polymerization in the absence of protein, Nature 374 (1995) 269–271.
[39] P. Gans, A. Sabatini, A. Vacca, Investigation of equilibria in solution. Determination of equilibrium constants with the hyperquad suite of programmes, Talanta 43 (1996) 1739–1753.
[40] S.R. Meshnick, Chloroquine as intercalator: a hypothesis revived, Parasitol. Today 6 (1990) 77–79.
[41] W.D. Wilson, R.L. Jones, Intercalating drugs: DNA binding and molecular pharmacology, Adv. Pharmacol. Chemother. 18 (1981) 177–222.
[42] N. Kumari, B.K. Maurya, R.K. Koiri, S.K. Trigun, S. Saripella, M.P. Coogan, L. Mishra, Cytotoxic activity, cell imaging and photocleavage of DNA induced by a Pt(II) cyclophane bearing 1,2 diamino ethane as a terminal ligand, MedChemComm 2 (2011) 1208–1216.
[43] S.N. Cohen, K.L. Yielding, Spectrophotometric studies of the interaction of chloroquine with deoxyribonucleic acid, J. Biol. Chem. 240 (1965) 3123–3131.
[44] E.T. Mudasir, D.H. Wahyuni, N. Tjahjono, H. Yoshioka, Inoue, Spectroscopic studies on the thermodynamic and thermal denaturation of the CT-DNA binding of methylene blue, Spectrochim. Acta Part A 77 (2010) 528–534.
[45] W. Trager, J.B. Jensen, Human malaria parasite in continuous culture, Science 193 (1976) 673–675.
[46] M.T. Makler, J.M. Ries, J.A. Williams, J.E. Bancroft, R.C. Piper, B.L. Gibbins, D.J. Hinrichs, Parasite lactate dehydrogenase as an assay for *Plasmodium falciparum* drug sensitivity, Am. J. Trop. Med. Hyg. 48 (1993) 739–741.